DALTON
FULL PAPER

Low-spin manganese(II) and cobalt(III) complexes of *N*-aryl-2-pyridylazophenylamines: new tridentate N,N,N-donors derived from cobalt mediated aromatic ring amination of 2-(phenylazo)pyridine. Crystal structure of a manganese(II) complex †

Amrita Saha, Partha Majumdar and Sreebrata Goswami *

Department of Inorganic Chemistry, Indian Association for the Cultivation of Science, Calcutta 700 032, India. Fax: 91-33-473 2805; E-mail: icsg@mahendra.iacs.res.in

Received 13th December 1999, Accepted 6th April 2000

Two new tridentate ligands of the type $NH_4C_5N{=}NC_6H_4N(H)C_6H_4(R)$ (R = H (HL^1) or CH_3 (HL^2)) have been synthesized by the cobalt mediated direct phenyl ring amination of co-ordinated $NH_4C_5N{=}NC_6H_5$. These bind to metal ions as monoanionic N,N,N-donors (L^-), affording $[Mn^{II}L_2]$ and $[Co^{III}L_2]ClO_4$ complexes in very high yields. The compounds have low-spin electronic configurations. While the manganese complexes are paramagnetic with one unpaired electron (1.65–1.70 μ_B) the cobalt complexes are diamagnetic. Crystal structure determination of $[Mn(L^1)_2]$ has revealed the presence of a distorted octahedral MnN_6 co-ordination sphere. The two aza nitrogens of the anionic tridentate ligands approach the metal centre closest with Mn–N(aza) *ca*. 1.89 Å. The other two Mn–N distances are: Mn–N(py), 2.00; Mn–N(amido), 1.95 Å. There is a significant degree of ligand backbone conjugation in the co-ordinated ligands which has resulted in shortening of the C–N bond distances and also in lengthening of the diaza (N=N) distances. In fluid solution, $[MnL_2]$ species exhibit six line EPR spectra with low hyperfine constant (A = 75 G). In frozen dichloromethane–toluene (77 K), rhombic EPR spectra are observed, consisting of an isolated signal g_3 (*ca*. 1.91) and two relatively close signals g_1 and g_2 (*ca*. 2.06 and 2.03 respectively). Both manganese as well as cobalt complexes display multiple redox responses. The manganese complexes show $Mn^{II} \rightleftharpoons Mn^{III}$ oxidation at *ca*. 0.38 V and the cobalt analogues display reversible $Co^{III} \rightleftharpoons Co^{II}$ reduction at −0.40 V. Electrogenerated $[Mn^{III}L_2]^+$ shows transitions in the near IR region.

Introduction

The low spin state ($S = \frac{1}{2}$) of manganese(II) is generally an uncommon entity[1–5] because of its highest spin-pairing energy[6] amongst bivalent 3d ions. Ligands with very strong ligand fields can induce low-spin character on this metal ion. Herein we describe a few low-spin manganese(II) and cobalt(III) complexes of a new anionic tridentate N,N,N donor (L^-). The low-spin complexes are of type $[Mn^{II}N_6]$ and $[Co^{III}N_6]^+$. The crystal structure of one member of the manganese complexes has been determined. Spectroelectrochemistry of each of these characterizes the existence of corresponding trivalent manganese and bivalent cobalt complexes in solutions.

The ligand 2-(2-(arylamino)phenyl)azopyridine (HL) was obtained[7] from an unusual cobalt-promoted fusion of aromatic amines to the pendant aryl ring of co-ordinated 2-(phenylazo)pyridine. It readily loses one H^+ and binds as a tridentate monoanionic donor. This report constitutes the first exploration of the co-ordination chemistry of this ligand which appears to be rich and versatile.

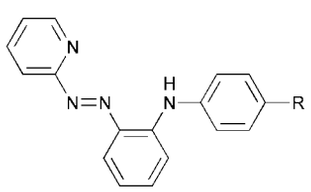

HL

R = H HL^1

R = Me HL^2

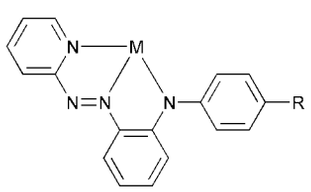

ML

Results and discussion

A. Ligand synthesis

(i) Cobalt-promoted aromatic ring amination of co-ordinated 2-(phenylazo)pyridine (pap). The neutral N,N-donor pap is known[8] to form a brown cationic tris chelate $[Co(pap)_3]^{2+}$ which reacts smoothly with neat $ArNH_2$ to produce[7] a green cobalt(III) complex, $[Co(L)_2]^+$, $[\mathbf{1}]^+$ (eqn. (1)). The cationic complex was isolated as its perchlorate salt in >80% yield.

$$[Co^{II}(pap)_3]^{2+} \xrightarrow{ArNH_2} [Co^{III}L_2]^+ \quad (1)$$

Brown → Green, $[\mathbf{1}]^+$

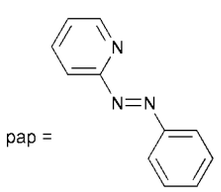

pap =

$ArNH_2$	$[CoL_2]^+$
aniline	$[\mathbf{1a}]^+$
p-toluidine	$[\mathbf{1b}]^+$

† Supplementary data available: ^{1}H NMR spectrum of HL^1 in $CDCl_3$, available from BLDSC (SUPP. NO. 57703, 2 pp.). See Instructions for Authors, Issue 1 (http://www.rsc.org/dalton).

DOI: 10.1039/a909769d

(ii) Isolation of HL from [1]$^+$ and its characterization. The reduction of cationic complex **[1]**$^+$ by dilute N_2H_4 followed by removal of Co^{2+} as CoS led to the isolation of HL in moderate yield (*ca.* 60%) (Scheme 1). The ligands HL were obtained as

$$[\mathbf{1}]^+ \xrightarrow{N_2H_4} [\mathbf{1}] \xrightarrow{(NH_4)_2S_x} HL + CoS$$

Scheme 1

crystalline orange solids which melt between 82 and 84 °C. The ligands, HL^1 and HL^2 showed resolved ^1H NMR in $CDCl_3$. The N–H resonance appeared[9] as a broad signal at δ 10.58. The four pyridyl protons resonate[10] in the range δ 7.5 to 8.7. Signals due to the rest of the aryl protons appear as overlapping resonances between δ 6.85 and 7.40. The ^1H NMR spectrum of HL^1 is deposited as supplementary material.

The solution spectrum of HL in CH_3CN consists of a strong absorption at 470–490 nm which is associated with two more transitions at 280 and 320 nm respectively. While the lowest energy transition[11] is due to n ⟶ π*, the rest are π ⟶ π* transitions. For comparison, the parent ligand pap shows[12] two transitions at 445 and 320 nm respectively. The ligand HL can be deprotonated very easily. The pK_a for HL^1 is quite low, 8.5, and the ligand $[L]^-$ binds as an anionic N,N,N-donor through the deprotonation of amine nitrogen. Notably, the 2-(phenylazo)pyridine part of $[L]^-$ is a strong acid[12] (soft) while the co-ordinating nitrogen of the $[NAr]^-$ part is a hard base. Thus the combination of the soft and hard donor characters of different binding sites in $[L]^-$ is capable of stabilizing transition metal ions in different oxidation states.

B. Low spin $[Mn^{II}(L)_2]$ and $[Co^{III}(L)_2]ClO_4$

(i) Isolation and characterization. The 2:1 reaction of HL with manganese(II) chloride tetrahydrate in methanol containing NEt_3 furnished dark brown $[Mn^{II}(L)_2]$ **2** in excellent yields (80–85%). The cationic green cobalt(III) complexes were similarly obtained from cobalt(II) chloride hexahydrate (eqn. (2)).

$$MCl_2{\cdot}nH_2O + 2HL \xrightarrow[NEt_3]{\text{methanol}} [M(L)_2]^{z+} \qquad (2)$$

M	z	Compound
Co^{III}	1	**[1]**$^+$
Mn^{II}	0	**2**

These cationic cobalt complexes were isolated as their perchlorate salts in almost quantitative yields. In solution, while the manganese(II) complexes are non-electrolytes, the cobalt complexes behave as 1:1 electrolytes (Λ = 120–130 Ω^{-1} cm^2 mol^{-1} in acetonitrile).

The cobalt complexes are diamagnetic and the room temperature (298 K) magnetic moments of solid $[Mn(L)_2]$ lie in the range 1.65–1.70 μ_B. Thus, both the species are low spin, idealized t_2^6 (Co^{III}) and t_2^5 (Mn^{II}). For comparison, the magnetic moments of low spin manganese(II) complexes are known to span the range[1–5] 1.7 to 2.3 μ_B. The diamagnetic cobalt(III) complexes exhibited highly resolved ^1H NMR spectra. In contrast the $[Mn(L)_2]$ complexes are EPR active. In fluid solution each of the complexes **2a** and **2b** exhibits a six-line (^{55}Mn, I = 5/2) spectrum with g = 2.043 and 2.058 respectively. A notable feature of the spectra is the relatively low value of the hyperfine coupling constant A, 70–85 G, which is characteristic[1] of a low spin state of Mn^{II}. For example, the A values for Mn^{II}(RxL) [H_2RxL = HON=C(R)N=$NC_6H_4S(CH_2)_xSC_6H_4$N=NC(R)=NOH (x = 2 or 3; R = Ph or α-naphthyl)] are *ca.* 70 G and those for other reported complexes[3b,c,4a,5] span the range 75–100 G. Thus the hyperfine coupling constants for the present manganese(II) complexes lie in the lower limit of the above range. This is expected due to strong dπ–pπ M–L interactions. In frozen (77 K) dichloromethane–toluene solution the $[Mn(L^1)_2]$ complex displays a well resolved rhombic spectrum. The EPR data are collected in Table 1 and representative spectra of **2a** are shown in Fig. 1. The three g components for the spectra of both **2a** and **2b** at 77 K further split due to hyperfine coupling to give complex spectral features characteristic of the low spin state of the manganese(II) complexes. These spectral features can be contrasted[13] with those of high spin manganese(II) complexes which show only very broad room temperature spectra spreading over g = 2–5 and very complex low temperature (77 K) spectra over a very wide range due to zero field splitting in the distorted metal environment. In no case ^{55}Mn hyperfine splitting is observable.

Table 1 EPR g values[a] and derived energy parameters of $[Mn(L)_2]$

Compound	g_1	g_2	g_3	Derived energy parameters[b]/cm^{-1} Δ	V	ΔE_1	ΔE_2
$[Mn(L^1)_2]$	2.043	2.022	1.897	1490	200	1375	1710
$[Mn(L^2)_2]$	2.057	2.033	1.916	1660	280	1510	1900

[a] In dichloromethane–toluene glass at 77 K. [b] Taking the value of the spin–orbit coupling constant (λ) for low-spin manganese(II) as equal to 300 cm^{-1}.

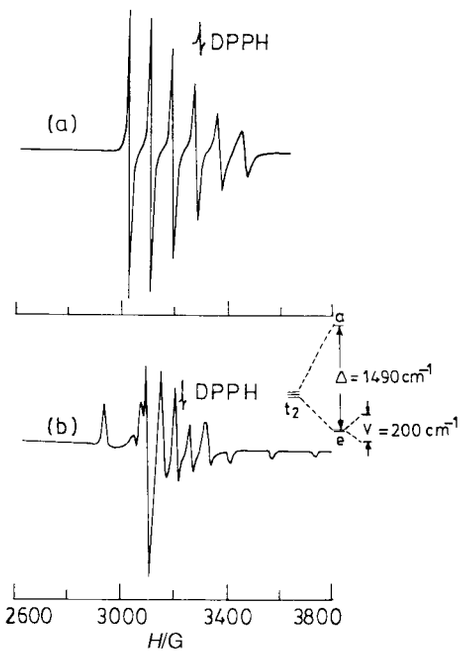

Fig. 1 EPR spectra of $[Mn(L^1)_2]$ in (a) 1:1 dichloromethane–toluene solution at 300 K, (b) frozen 1:1 dichloromethane–toluene solution at 77 K, showing computed splittings of t_2 orbitals. DPPH = Diphenylpicrylhydrazyl.

The rhombicity of the EPR spectra in the present cases indicates[14] the asymmetry of the electronic environment around manganese(II) in the $[Mn(L)_2]$ complexes. The spectra may be considered as pseudo-axial, consisting of a rather isolated signal g_3 ($g_\parallel$ in the true axial case) and two relatively close signals g_1 and g_2 (rhombic components of $g_\perp$). Accordingly, the axial distortion (Δ), that splits t_2 levels into a and e components, is expected to be larger than the rhombic distortion (V), which splits e (Fig. 1). Spin–orbit coupling causes further changes in the energy gap. Thus, two electronic transitions (transition energies ΔE_1 and ΔE_2, $\Delta E_1 < \Delta E_2$) are, in principle, probable within these three levels. All these energy parameters have been computed (Table 1) using the observed g values, the g-tensor theory[15] of low-spin d^5 complexes and a reported method.[16] The axial distortion is indeed much stronger than the rhombic

Table 2 Selected bond lengths (Å) for $[Mn(L^1)_2]$

Mn–N(1)	2.003(2)	N(8)–C(29)	1.424(3)
Mn–N(3)	1.8877(19)	C(23)–C(24)	1.395(3)
Mn–N(4)	1.957(2)	C(24)–C(25)	1.369(4)
Mn–N(5)	1.997(2)	C(25)–C(26)	1.394(4)
Mn–N(7)	1.8894(19)	C(26)–C(27)	1.368(4)
Mn–N(8)	1.950(2)	C(27)–C(28)	1.411(4)
N(5)–C(22)	1.361(3)	N(5)–C(18)	1.351(3)
N(6)–C(22)	1.362(3)	C(18)–C(19)	1.370(4)
N(6)–N(7)	1.324(3)	C(19)–C(20)	1.383(4)
N(7)–C(23)	1.388(3)	C(20)–C(21)	1.359(4)
C(23)–C(28)	1.410(3)	C(21)–C(22)	1.399(4)
C(28)–N(8)	1.357(3)		

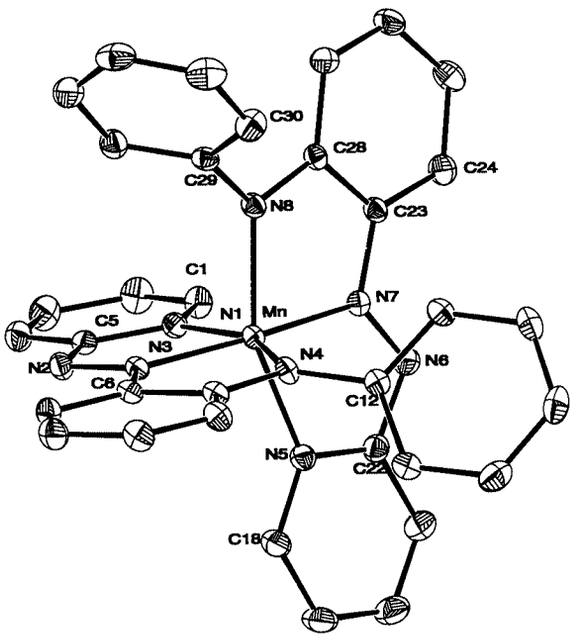

Fig. 2 An ORTEP[17] diagram of $[Mn(L^1)_2]$, **2a**.

one. The calculated values of ΔE_1 and ΔE_2 are 1375–1510 and 1710–1900 cm^{-1} respectively which lie in the infrared region and could not be detected. The analysis of EPR spectral data thus indicates that the $[Mn(L)_2]$ complexes are significantly distorted from an ideal octahedral arrangement. This is further revealed from the structural analysis as discussed below.

(ii) Structure of $[Mn(L^1)_2]$. Fig. 2 shows the molecular structure of the complex $[Mn(L^1)_2]$ along with the atomic numbering scheme used. Selected bond distances are listed in Table 2. The two ligands bind the metal in the N_6 fashion using pairs of pyridyl-N, azo-N, and amido-N atoms. The relative orientations within the pairs are *cis*, *trans* and *cis*, respectively. The chelate bite angles N(py)–Mn–N(azo), *i.e.* N(1)–Mn–N(3) and N(5)–Mn–N(7), are similar (*ca.* 77°) and smaller than N(azo)–Mn–N(amido) bite angles (*ca.* 81°). The corresponding cobalt(III) complex also showed[7] a similar trend. The two aza nitrogens of the anionic tridentate ligands approach the metal centre closest, with Mn–N(3)/N(7) *ca.* 1.89 Å. The Mn–N(py) (*ca.* 2.00 Å) distances are longest.

There is an indication of significant backbone conjugation in the co-ordinated anionic ligand. The average distance N(aza)–C(phenyl) 1.38 Å is shorter than the value of 1.421(5) Å found for the corresponding distance[18] in the salt $[Hpap]ClO_4$. Similarly, the amido nitrogen of $[L]^-$ binds to the phenyl group of pap at a shorter distance than is found for a N–C(phenyl) single bond distance. The N=N aza distances also indicate elongation which is consistent with the notion of greater electron delocalization along the ligand backbone in the anionic $[L]^-$. Some degree of conjugation along the ligand backbone of the bischelate system could be implicated in the shortening of the Mn–N(aza) bonds, either through an increase in the electron density on N(aza) and a concomitant increased basicity or through enhanced π-bonding capability of the more conjugated ligand.

Table 3 Cyclic voltammetric data[a]

Compound	Oxidation $E_{1/2}$/V	Reduction $-E_{1/2}$/V
$[Mn(L^1)_2]$	0.38, 1.10,[b] 1.56[c]	0.96, 1.45, 1.88[d]
$[Mn(L^2)_2]$	0.35, 1.05,[b] 1.52[c]	0.98, 1.47, 1.89[d]
$[Co(L^1)_2]ClO_4$	1.21,[b] 1.56[c]	0.40, 0.81, 1.52[d]
$[Co(L^2)_2]ClO_4$	1.17,[b] 1.51[c]	0.41, 0.80, 1.49[d]
HL^1	1.05,[c] 1.36[c]	1.11, 1.51[d]

[a] Experiments were carried out in CH_3CN and CH_2Cl_2 at 298 K using NEt_4ClO_4 as supporting electrolyte. The reported data correspond to a scan rate of 50 mV s^{-1}. [b] $i_{pa} > i_{pc}$. [c] Irreversible anodic response; the potential corresponds to E_{pa}. [d] Irreversible cathodic response; the potential corresponds to E_{pc}.

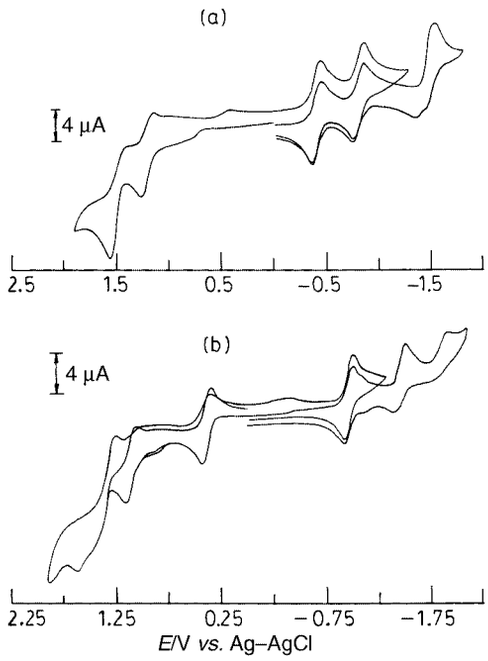

Fig. 3 Cyclic voltammograms (scan rate 50 mV s^{-1}) of a 10^{-3} M solution in acetonitrile (0.1 M NEt_4ClO_4) at 298 K at a platinum working electrode of (a) $[Co(L^1)_2]^+$, (b) $[Mn(L^1)_2]$.

C. Redox and spectroelectrochemistry

Redox properties of the cobalt and manganese complexes have been studied by cyclic voltammetry (CV) using a platinum working electrode. Voltammetric data are collected in Table 3 and representative voltammograms are shown in Fig. 3.

The cobalt complexes, $[\mathbf{1}]^+$, display three major reversible to quasireversible cathodic responses in the range −0.0 to −1.5 V. These also show two high potential (>1.0 V) anodic responses, of which the first is quasireversible ($i_{pa} > i_{pc}$) and the other one is irreversible. The manganese complexes **2**, on the other hand, show a low potential anodic response at *ca.* 0.38 V in addition to two high potential responses occurring at similar potentials to those for the cobalt analogues. The cathodic scans for **2** show one reversible response at −0.96 V which lies in between the second and third cathodic responses for the cobalt complex. It may be worthwhile first to consider the redox potentials of a representative "free" ligand, *viz.* HL^1. It displays two irreversible anodic and a reversible cathodic response at 1.05, 1.36, and −1.11 V respectively (Table 3). A comparison of the nature of the voltammograms of $[Co(L^1)_2]^+$, $[Mn(L^1)_2]$, and HL^1 confirms that the first cathodic response for the cobalt complex and the least potential anodic response for the manganese complex

Table 4 Electronic spectral data

Compound	Absorption[a] λ_{max}/nm(ε/M^{-1} cm^{-1})
$[Mn(L^1)_2]$	1170(2060), 760(10360), 575(10940), 525[b](9360), 375(15030), 322[b](25300), 290(32320), 240(40430)
$[Mn(L^1)_2]^{+}$[c]	2390[b](1270), 2260[b](2220), 2230[b](2380), 1750[b](1110), 745[b](5546), 640(13310), 515(11410), 400[b](15700), 325[b](24250)
$[Mn(L^1)]^{-}$[c]	680[b](7610), 580[b](7290), 535[b](6500), 340(24900), 300(24560)
$[Mn(L^2)_2]$[d]	760(11340), 575(11800), 523[b](10040), 370(10180), 320[b](27700), 290(34060), 245(43110)
$[Co(L^1)_2]PF_6$	885(7650), 795(11460), 715(10550), 650[b](8600), 400[b](17474), 375[b](17600), 310[b](22170), 250(48140)
$[Co(L^1)_2]$[c]	800[b](7450), 730[b](6880), 525[b](5160), 475(9740), 395[b](17770), 420(18340), 255(41840)
$[Co(L^1)_2]^{-}$[c]	970[b](3440), 890[b](4580), 860[b](4580), 630[b](4580), 500[b](9740), 408(25790), 295[b](30950), 260(40120)
$[Co(L^2)_2]ClO_4$[d]	795(10600), 720(10300), 660[b](8580), 375[b](21580), 350[b](21000), 320[b](21700), 250(46500)
HL^1[d]	490(7820), 420[b](5640), 325(15800), 280(19800), 220[b](23800)
HL^2[d]	495(7970), 325(15100), 280(18210), 220[b](15370), 215(16520)

[a] Data obtained from absorption spectra: solvent CH_3CN. [b] Shoulder. [c] Spectroelectrochemically generated compound in an OTTLE cell (see text). [d] Spectral data in UV and visible range.

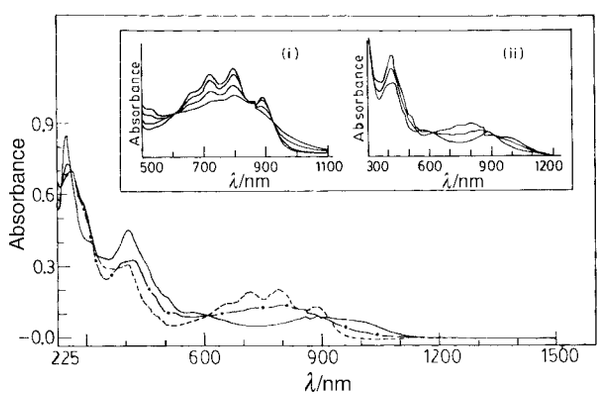

Fig. 4 Solution spectra of $[Co(L^1)_2]^{+}$ (- - - -), $[Co(L^1)_2]$ (– · –) and $[Co(L^1)_2]^{-}$ (——). Inset: OTTLE cell experiments, time dependence spectra, applied potential −0.65 (i), −1.0 V (ii).

may be assigned to $Co^{III} \rightleftharpoons Co^{II}$ and $Mn^{II} \rightleftharpoons Mn^{III}$ redox couples in the respective complexes. The nature of the other responses is not certain and may be due to redox processes at the co-ordinated $[L]^{-}$ centres.

In order to study the spectra of the electrogenerated cobalt(II) and manganese(III) complexes, two representative examples *viz.* $[Co(L^1)_2]ClO_4$ and $[Mn(L^1)_2]$ were chosen for spectroelectrochemical studies. These were performed in an optically transparent thin layer electrode (OTTLE) cell. The compounds are more soluble in dichloromethane (dcm) than in acetonitrile and hence dcm was used as the solvent for a meaningful record of relatively low intensity spectral changes especially in the low energy region. It is to be noted here that the nature as well as the potentials of the redox responses of both the above cobalt(III) and manganese(II) complexes are similar in these two solvents.

Fig. 4 shows the solution spectra of $[Co(L^1)_2]^{+}$ $[\mathbf{1}]^{+}$ along with electrogenerated $[Co(L^1)_2]$ **1** and $[Co(L^1)_2]^{-}$ $[\mathbf{1}]^{-}$. The spectral data are collected in Table 4. Both reduction processes are reversible and the spectra of the starting cationic $[\mathbf{1}]^{+}$, neutral **1**, and anionic $[\mathbf{1}]^{-}$ compounds may quantitatively be reproduced by application of the appropriate potentials. The starting complex shows an envelope of four closely spaced transitions in

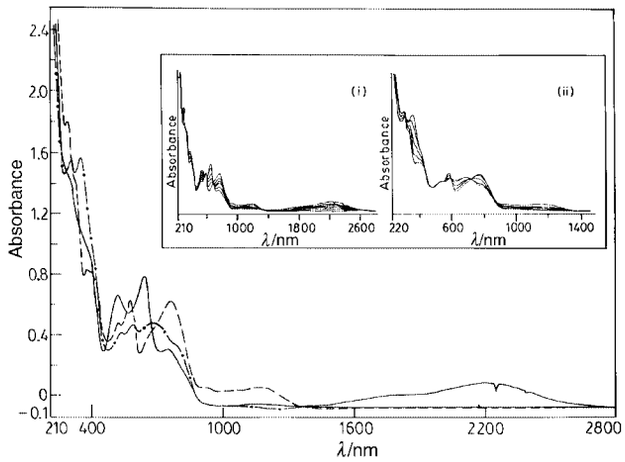

Fig. 5 Solution spectra of $[Mn(L^1)_2]$ (- - - -), $[Mn(L^1)_2]^{+}$ (——) and $[Mn(L^1)_2]^{-}$ (– · –). Inset: OTTLE cell experiments, time dependence spectra, applied potential 0.75 (i), −1.30 V (ii).

the range 900–650 nm. On the basis of their high intensities, these transitions are assigned as charge transfer in nature. Since, Co^{III} in complex $[\mathbf{1}]^{+}$ is in the low-spin t_2^6 configuration, these low energy bands may be due[19] to $d\pi(Co^{III})$ to ligand acceptor orbitals. The multiple nature of the transitions originates from the lack of symmetry of the co-ordination environment as well as the presence of different acceptor levels. Upon successive reductions, $[\mathbf{1}]^{+} \longrightarrow \mathbf{1} \longrightarrow [\mathbf{1}]^{-}$, the transition energies as well as the intensities both decrease appreciably (Table 4). However, the intensities are still high for allowed charge transfer transitions. This may be due to considerable mixing of metal and ligand orbitals. There are two more major transitions at 400 and 250 nm. This part of the spectrum (400–220 nm) of $[Co(L^1)_2]^{+}$ closely matches with the spectrum of $[Mn(L^1)_2]^{+}$ (see below). These transitions may be assigned as intra-ligand transitions. The "free" ligand HL^1 shows multiple transitions in the region 500–220 nm. Its conjugate base, $[L]^{-}$, generated in solution by the addition of dilute NaOH(aq) showed almost identical spectral features.

The transitions in the range 1400–450 nm for the manganese(II) complex $[Mn(L^1)_2]$ are vastly different from those observed for $[Co(L^1)_2]^{+}$. The lowest energy transition at 1170 nm is broad and least intense (ε 2060 M^{-1} cm^{-1}). There are three more highly intense (ε >10000 M^{-1} cm^{-1}) major transitions in the aforesaid region. Upon oxidation of **2a** to $[\mathbf{2a}]^{+}$, the 1170 nm transition disappeared with concomitant appearance of two broad transitions at 1750 and 2260 nm. These transitions may be assigned to partially allowed transitions originating[20] from the splitting of low-spin d^4 Mn^{III}. However, the intensities of these are very high as compared to usual d–d transitions which may be attributed to considerable mixing of metal and ligand orbitals. Upon reduction of the starting manganese(II) complex the broad low energy transition disappeared. The visible range spectra of the manganese complexes consist of multiple intense charge transfer transitions. The bivalent complex, **2a**, showed two major transitions at 760 and 575 nm respectively which may be assigned as metal to ligand charge transfer $[d\pi(Mn^{II}) \rightarrow L]$. Upon oxidation to the corresponding trivalent state $[\mathbf{2a}]^{+}$ these two transitions are blue shifted. The UV-range transitions are dominated by strong intra-ligand charge transfer. The spectral changes due to oxidation and reduction of $[Mn(L^1)_2]$ are shown in Fig. 5.

Conclusion

We have successfully achieved the synthesis of some new low-spin manganese(II) and cobalt(III) complexes. The ligands (HL) used in this work are obtained from novel cobalt assisted

organic ring amination processes *via* C–H activation. The presence of the combination of hard and soft binding sites in these N,N,N-donors makes them excellent ligands for soft as well as hard metal ions. The bond distances in the manganese complexes are indicative of extensive delocalization along the ligand backbone. This effect is also reflected in the unusual low hyperfine constant, A, values in their EPR spectra. The metal oxidation potentials for $[MnL_2]$ are low. The spectroelectrochemical studies on $[MnL_2] \rightleftharpoons [MnL_2]^+$ and $[Co(L)_2]^+ \rightleftharpoons [Co(L)_2]$ redox processes confirm the existence of the corresponding trivalent manganese and bivalent cobalt complexes respectively in solution. The co-ordination chemistry involving anionic $[L]^-$ appears to be very rich with many uncommon features which are under scrutiny.

Experimental

Materials

The starting complex $[Co(pap)_3][ClO_4]_2$ was prepared by the reported method.[8] Solvents and chemicals used for synthesis were of analytical grade. The supporting electrolyte tetraethylammonium perchlorate and solvents for electrochemical work were obtained as before.[21] **CAUTION**: perchlorate salts of metal complexes are generally explosive. Although no detonation tendencies have been observed, care is advised and handling of only small quantities recommended.

Physical measurements

A Shimadzu UV 21000 uv/vis spectrophotometer was used to record electronic spectra. The IR spectra were obtained with a Perkin-Elmer 783 spectrophotometer, ^{1}H NMR spectra in $CDCl_3$ with a Bruker Avance DPX300 spectrophotometer and $SiMe_4$ as internal standard. A Perkin-Elmer 240C elemental analyser was used to collect microanalytical data (C,H,N). Electrochemical measurements were performed under a dry nitrogen atmosphere on a PAR model 370-4 electrochemistry system as described earlier.[18] All potentials reported in this work are referenced to the Ag–AgCl electrode and uncorrected for junction contribution. The pH measurements were made with a μ-pH system 361 Systronics pH meter, standardized with buffers 7.0 and 9.2. Electrical conductivities were measured by using a Systronic Direct Reading Conductivity meter 304. The pK value was determined pH-metrically as described before.[22] EPR measurements were made with a Varian 109C E-line X-band spectrometer fitted with a flat cell. Spectra were calibrated with DPPH ($g = 2.0037$). Magnetic moment measurements were carried out by using a PAR 155 vibrating sample magnetometer fitted with a Walker Scientific L75FBAL magnet. Spectroelectrochemical studies were carried out in an OTTLE cell mounted in the sample compartment of a Perkin-Elmer Lambda 19 spectrophotometer, as described earlier.[23]

Syntheses

Bis{phenyl[2-(2-pyridylazo)phenyl]amido}cobalt(III) perchlorate, $[Co(L^1)_2]ClO_4$, [1a]$^+$. A mixture of $[Co(pap)_3][ClO_4]_2$ (0.2 g, 0.248 mmol) and aniline (0.5 ml) was heated on a steam bath for 1 hour. The initial brown colour gradually changed to intense green. The cooled green mixture was throughly washed with diethyl ether. Crystallization of the crude product from a dichloromethane–hexane mixture yielded **[1a]**$^+$ (83%) as green crystals. Found: C, 57.35; H, 3.86; N, 15.45. Calc. for $C_{34}H_{26}ClCoN_8O_4$: C, 57.92; H, 3.69; N, 15.89%. $\Lambda_M = 120\ \Omega^{-1}\ cm^2\ mol^{-1}$ (1×10^{-3} M in CH_3CN). IR(KBr): ν(N=N) 1250, ν(C–N) 1590, $\nu(ClO_4^-)$ 1100, 625 cm^{-1}.

The complex $[Co(pap)_3][ClO_4]_2$ reacts similarly with *p*-toluidine to yield crystalline $[Co(L^2)_2]ClO_4$, **[1b]**$^+$. Yield (80%). Found: C, 58.93; H, 3.90; N, 14.91. Calc. for $C_{36}H_{30}ClCoN_8O_4$: C, 58.98; H, 4.09; N, 15.29%. $\Lambda_M = 130\ \Omega^{-1}\ cm^2\ mol^{-1}$ (1×10^{-3} M in CH_3CN). IR(KBr): ν(N=N) 1240, ν(C–N) 1590, $\nu(ClO_4^-)$ 1090, 620 cm^{-1}.

Isolation of 2-[2-(phenylamino)phenyl]azopyridine (HL^1) from complex [1a]$^+$. The compound $[Co(L^1)_2]ClO_4$ (0.0834 g, 0.1184 mol) was dissolved in ethanol (30 ml) and to it hydrazine hydrate (5 ml) and yellow ammonium sulfide (5 ml) were added. The mixture was then stirred for 30 min at room temperature. The resulting orange-yellow solution was evaporated under vacuum, then extracted with benzene and subjected to column chromatography on a silica gel (1×15 cm) column. An orange-yellow band was eluted with benzene–chloroform (90 : 10), which on evaporation yielded orange crystals of HL^1 in 60% yield. Found: C, 74.09; H, 5.38; N, 19.36. Calc. for $C_{17}H_{14}N_4$: C, 74.45; H, 5.10; N, 20.43%. IR(KBr): ν(N=N) 1240, ν(C–N) 1595 cm^{-1}. mp 82 °C. p$K_a = 8.5 \pm 1$. ^{1}H NMR: δ 10.58 (N–H), 8.70 (d, 4 H), 8.00 (d, 1 H), 7.87 (t, 2 H), 7.15 (t, 7 H), 6.90 (t, 8 H) and 7.77 (d, 9 H).

Similarly, **HL^2** was isolated as orange needles from $[Co(L^2)_2]ClO_4$, **1b**. Yield 58%. Found: C, 75.26; H, 5.73; N, 19.55. Calc. for $C_{18}H_{16}N_4$: C, 75.00; H, 5.55; N, 19.44%. IR(KBr): ν(N=N) 1240, ν(C–N) 1510 cm^{-1}. mp 84 °C. p$K_a = 7.5 \pm 1$. ^{1}H NMR: 10.58 (N–H), 8.70 (d, 4 H), 8.00 (d, 1 H), 7.88 (t, 2 H), 7.35 (t, 7 H), 6.90 (t, 8 H) and 7.80 (d, 9 H).

$[Co(L^1)_2]ClO_4$ from preformed HL^1. The ligand HL^1 (0.157 g, 0.573 mmol) was dissolved in 25 ml of methanol and to it 1–2 drops of triethylamine were added. To the deprotonated ligand solution a methanolic solution of $CoCl_2 \cdot 6H_2O$ (0.06819 g, 0.287 mmol) was added and the mixture stirred for 1 hour at room temperature. The solution changed from orange-yellow to green. The resulting solution was filtered and to it diluted aqueous $NaClO_4$ was added. The dark crystalline compound thus obtained was recrystallized from dichloromethane–hexane. Yield 93%. The physicochemical properties of this compound exactly correspond to those of an authentic sample obtained from the reaction of $[Co(pap)_3]^{2+}$ and $PhNH_2$ as described above.

The complex $[Co(L^2)_2]ClO_4$ **[1b]**$^+$ was obtained similarly in 95% yield by treating HL^2 with hydrated cobalt(II) chloride.

Bis{phenyl[2-(2-pyridylazo)phenyl]amido}manganese(II), $[Mn(L^1)_2]$ 2a. The ligand HL^1 (0.1455 g, 0.53 mmol) was dissolved in 25 ml of methanol and to it 1–2 drops of triethylamine were added. To the deprotonated ligand solution a methanolic solution of $MnCl_2 \cdot 4H_2O$ (0.06834 g, 0.26 mmol) was added and the mixture stirred for 1 hour at room temperature. The solution changed from orange-yellow to dark brown. The resultant mixture was filtered and the solvent evaporated under vacuum. The compound thus obtained was finally crystallized from dichloromethane–hexane. Yield 85%. Found: C, 67.58; H, 4.42; N, 18.70. Calc. for $C_{34}H_{26}MnN_8$: C, 67.89; H, 4.32; N, 18.63%. μ_{eff} (298 K): 1.65 μ_B. IR(KBr): ν(N=N) 1230, ν(C–N) 1590 cm^{-1}.

Similarly $MnCl_2 \cdot 4H_2O$ reacted with HL^2 in 1 : 2 ratio in methanolic solution in the presence of 1–2 drops of triethylamine as base to give crystalline $[Mn(L^2)_2]$ **2b**. Yield 80%. Found: C, 68.48; H, 5.26; N, 17.56. Calc. for $C_{36}H_{30}MnN_8$: C, 68.68; H, 4.77; N, 17.80%. μ_{eff} (298 K): 1.70 μ_B. IR(KBr): ν(N=N) 1230, ν(C–N) 1595 cm^{-1}.

Crystal structure of $[Mn(L^1)_2]$ 2a

An X-ray quality crystal of complex **2a** was obtained by slow diffusion of a dichloromethane solution of the compound into hexane. The crystal data are collected in Table 5. Intensity data for a brown cubic crystal with dimensions $0.51 \times 0.48 \times 0.47$ mm were measured on an Enraf-Nonius MACH3 automatic diffractometer equipped with graphite-monochromated Mo-Kα

Table 5 Crystallographic data and details of refinement of $[Mn(L^1)_2]$

Chemical formula	$C_{34}H_{26}MnN_8$
Formula weight	601.57
T/K	293(2)
Crystal system	Monoclinic
Space group	$P2_1/n$
a/Å	10.3746(17)
b/Å	16.061(6)
c/Å	16.726(6)
β/°	90.15(2)
V/Å^3	2786.9(15)
Z	4
μ/mm^{-1}	0.514
Reflections collected/unique	5381/4901 [R(int) = 0.0000]
Final R indices [$I > 2\sigma(I)$]	$R1 = 0.0332$, $wR2 = 0.0740$

radiation, $\lambda = 0.71073$ Å. Data were corrected for Lorentz-polarization effects.[21] A total of 5381 reflections were collected, of which 4901 were unique and 3584 satisfied the $I > 2\sigma(I)$ criterion and were used in the subsequent analysis. The structure was solved by employing the SHELXS 86 program package[24] which revealed the positions of all non-hydrogen atoms, and refined by full-matrix least squares based on F^2.[25] All hydrogen atoms of the ligands were exactly located in calculated positions.

CCDC reference number 186/1928.

See http://www.rsc.org/suppdata/dt/a9/a909769d/ for crystallographic files in .cif format.

Acknowledgements

Financial support received from the Department of Science and Technology, New Delhi, is acknowledged. X-Ray data on complex **2a** were collected at the National Single Crystal X-Ray Facilities at the School of Chemistry, University of Hyderabad. We thank Dr S. Paul and Dr S. Bhattacharya for their help. SG is grateful to Professor J. A. McCleverty and Dr M. D. Ward for allowing him to perform the OTTLE cell experiments at their laboratory. He also thanks the RSC for its financial support which allowed him to visit the University of Bristol.

References

1 S. Ganguly, S. Karmakar, C. K. Pal and A. Chakravorty, *Inorg. Chem.*, 1999, **38**, 5984; S. Karmakar, S. B. Choudhury and A. Chakravorty, *Inorg. Chem.*, 1994, **33**, 6148; P. Basu and A. Chakravorty, *Inorg. Chem.*, 1992, **31**, 4980; P. Basu, S. Pal and A. Chakravorty, *Inorg. Chem.*, 1988, **27**, 1848.
2 U. Knof, T. Weyhermüller, T. Wolter and K. Weighardt, *J. Chem. Soc., Chem. Commun.*, 1993, 726.
3 (*a*) W. P. Griffith *Coord. Chem. Rev.*, 1975, **17**, 177; (*b*) P. T. Manoharan and H. B. Gray, *Chem. Commun.*, 1965, 324; (*c*) D. A. C. McNeil, J. B. Raynor and M. C. R. Symons, *J. Chem. Soc.*, 1965, 410.
4 (*a*) P. Fantucci, L. Naldini, F. Cariati, V. Valenti and C. Bussetto, *J. Organomet. Chem.*, 1974, **64**, 109; (*b*) D. S. Matteson and R. A. Bailey, *J. Am. Chem. Soc.*, 1969, **91**, 1975.
5 N. G. Connelly, K. A. Hassard, B. J. Dunne, A. G. Orpen, S. J. Raven, G. A. Carriedo and V. Riera, *J. Chem. Soc., Dalton Trans.*, 1988, 1623; G. A. Carriedo, V. Riera, N. G. Connelly and S. J. Raven, *J. Chem. Soc., Dalton Trans.*, 1987, 1769.
6 A. B. P. Lever, *Inorganic Electronic Spectroscopy*, 2nd edn., Elsevier, New York, 1984, p. 750.
7 A. Saha, A. K. Ghosh, P. Majumdar, K. N. Mitra, S. Mondal, K. K. Rajak, L. R. Falvello and S. Goswami, *Organometallics*, 1999, **18**, 3772.
8 A. K. Mahapatra, Ph.D. Thesis, Jadavpur University (India), 1989.
9 K. N. Mitra, S. Choudhury, A. Castiñeiras and S. Goswami, *J. Chem. Soc., Dalton Trans.*, 1998, 2901.
10 A. K. Mahapatra, B. K. Ghosh, S. Goswami and A. Chakravorty, *J. Indian Chem. Soc.*, 1986, **63**, 101.
11 K. C. Kalia and A. Chakravorty, *J. Org. Chem.*, 1970, **35**, 2231.
12 S. Goswami, A. R. Chakravarty and A. Chakravorty, *Inorg. Chem.*, 1981, **20**, 2246.
13 P. Chakravorty, S. K. Chandra and A. Chakravorty, *Inorg. Chem.*, 1993, **32**, 5349; R. Rajan, R. Rajaram, B. U. Nair, T. Ramasami and S. K. Mondal, *J. Chem. Soc., Dalton Trans.*, 1996, 2019.
14 P. H. Rieger, *Coord. Chem. Rev.*, 1994, **135/136**, 203.
15 B. Bleaney and M. C. M. O'Brien, *Proc. Phys. Soc. London, Sect. B*, 1956, **69**, 1216; J. S. Griffith, *The Theory of Transition Metal Ions*, Cambridge University Press, London, 1961, p. 364.
16 S. Bhattacharya and A. Chakravorty, *Proc. Indian Acad. Sci., Chem. Sci.*, 1985, **95**, 159.
17 C. K. Johnson, ORTEP II, Report ORNL-5138, Oak Ridge National Laboratory, Oak Ridge, TN, 1976.
18 P. Majumdar, S.-M. Peng and S. Goswami, *J. Chem. Soc., Dalton Trans.*, 1998, 1569.
19 B. K. Santra and G. K. Lahiri, *J. Chem. Soc., Dalton Trans.*, 1997, 1883.
20 F. A. Cotton, G. Wilkinson, C. A. Murillo and M. Bochmann, *Advanced Inorganic Chemistry*, 6th edn., John Wiley and Sons, Inc., New York, 1999, p. 764.
21 S. Choudhury, A. K. Deb and S. Goswami, *J. Chem. Soc., Dalton Trans.*, 1994, 1305.
22 P. Ghosh and A. Chakravorty, *J. Chem. Soc., Dalton Trans.*, 1985, 361.
23 S.-M. Lee, M. Marcaccio, J. A. McCleverty and M. D. Ward, *Chem. Mater.*, 1998, **10**, 3272.
24 G. M. Sheldrick, SHELXS 86, Program for the solution of crystal structures, University of Göttingen, 1993.
25 G. M. Sheldrick, SHELXL 97, Program for the refinement of crystal structure, University of Göttingen, 1997.